AJNR

Foci of MRI Signal (Pseudo Lesions) Anterior to the Frontal Horns: Histologic Correlations of a Normal Finding

Gordon Sze, Stephan J. De Armond, Michael Brant-Zawadzki, Richard L. Davis, David Norman and T. Hans Newton

Foci of MRI Signal (Pseudo Lesions) Anterior to the Frontal Horns: Histologic Correlations of a Normal Finding

Gordon Sze[1]
Stephan J. De Armond[2]
Michael Brant-Zawadzki[1]
Richard L. Davis[2]
David Norman[1]
T. Hans Newton[1]

Review of all normal magnetic resonance (MR) scans performed over a 12-month period consistently revealed punctate areas of high signal intensity on T2-weighted images in the white matter just anterior and lateral to both frontal horns. Normal anatomic specimens were examined with attention to specific characteristics of this region. Three unique features typify the brain tissues that correspond to the foci of high signal. First, this region of the brain is notable for its loose network of axons with low myelin content. Second, pathologic scrutiny revealed an entity called "ependymitis granularis," which represents patchy loss of the ependyma in the frontal horns with astrocytic gliosis. Third, flow of interstitial fluid within this region of the brain tends to converge at the dorsal-lateral angle of the frontal horns. All these factors contribute to increased water content locally, which results in foci of high signal intensity anterior to the frontal horns in all normal MR scans.

The unprecedented sensitivity of MR to altered tissue content has allowed superior detection of disease processes, even when clinically silent, and has also permitted hitherto undetected visualization of existing anatomic structures. This investigation focuses on foci of relatively high signal intensity just anterior to the frontal horns of the lateral ventricles bilaterally. These foci of high signal intensity on T2-weighted spin-echo images initially suggested disease [1], but because we saw them routinely we were prompted to do an autopsy study to provide a histologic explanation for the finding.

Materials and Methods

Patient Selection

The MR brain scans of all patients imaged at the University of California, San Francisco over a 1-year period were retrospectively reviewed, and 56 patients were selected for this study. All 56 patients had otherwise normal MR scans and were initially referred because of nonspecific, subjective symptoms.

Table 1 lists the symptoms for which the 56 patients were originally studied. None of the patients had any underlying systemic disease process that might predispose them to central nervous system (CNS) disease. Specifically, all patients referred for evaluation of possible multiple sclerosis or other demyelinating disease were excluded, even when their MR examination proved to be normal [2]. Patients with connective tissue disorders [3], dementia [4, 5], or neurologic signs (as opposed to symptoms) were also excluded.

CT scans usually were not done at our institution, but in all cases, the results of CTs performed elsewhere were either unremarkable or negative. The patients who were selected for our study ranged in age from 9 months to 82 years (Table 2).

Imaging

MRI was usually performed with a 0.35-T superconductive magnet and a 25-cm diameter head coil [6, 7, 8]. Multislice spin-echo acquisition was employed to obtain slices 7-mm thick.

TABLE 1: **Indications for Performance of MR Scans**

Reason for MR Study	No. of Studies
Seizures	12
Headache	11
Normal controls	10
Rule out primary intracranial tumor	8
Rule out extraaxial tumor	6
Dizziness or vertigo	6
Subjective sensory symptoms (e.g. numbness, without definite signs or anatomic distribution)	6
Rule out pituitary tumor	3
Facial spasm	3
Rule out metastases	2
Developmental delay	1
Dyslexia	1

Note:—The total number of studies done (69) exceeds the actual number of patients (56) because some patients complained of more than one symptom (e.g., headache and dizziness).

TABLE 2: **Ages of the Patients Included in the Study**

Age (years)	No. of Patients
0–10	6
11–20	7
21–30	6
31–40	6
41–50	6
51–60	7
61–70	8
71–80	6
81–90	2

A repetition time (TR) of 1.5 or 2 sec and echo-delay times of 28 and 56 msec were used. In addition, in many patients acquisitions with a TR of 0.5 sec were performed. Only axial images were reviewed in this study.

Later scans were also reviewed using a different MR imager with a 1.5-T superconductive magnet and a 24-cm diameter head coil. Multislice spin-echo acquisition was employed to obtain slices 1 cm thick. A repetition time of 2 sec, with echo-delay times of 40 and 80 msec, routinely showed the same finding.

Autopsy Review

For histologic correlation, approximately 150 specimens that were considered normal by the neuropathology division were selected. These patients had shown no evidence of CNS disease and their brains had been scrutinized with particular attention to the region surrounding the frontal horns. Retrospectively, 39 of these specimens were reexamined and new sections of the region in question were obtained. Selection of these patients was determined by age, with approximately 3 to 4 specimens chosen from each decade. Ages ranged from fetuses of 20 weeks gestation to adults 92 years old (Table 3).

Three different stains were used in the study: Luxol Fast Blue-Periodic Acid Schiff (LFB-PAS), which stains myelin blue; Biel-schowsky, an axonal stain; and Glial Filament Protein (GFAP), which stains for astrocytes.

TABLE 3: **Breakdown of Autopsy Specimens According to Age of Patient and Cause(s) of Death**

Age[a]	No. of Specimens	Cause of Death
20–30 weeks fetus	10	Therapeutic abortion
0–1 yr	3	Sepsis, congenital heart disease, epidermolysis bullosa
1–10	3	Cystic fibrosis, congenital heart disease
11–20	3	Leukemia, congenital heart disease
21–30	2	Cystic fibrosis, cardiomyopathy
31–40	3	Cardiomyopathy, carcinoma, cardiac arrest
41–50	3	Leukemia, upper gastrointestinal bleed, carcinoma
51–60	3	Carcinoma, coronary artery disease and renal failure
61–70	3	Congestive heart failure, ruptured aneurysm, respiratory failure
71–80	4	Ruptured aneurysm, coronary artery disease, idiopathic thrombocytopenic purpura
81–90	1	Arrhythmia
91–100	1	Sepsis
Total	39	

[a] Age in years, unless otherwise specified.

Results

The high-intensity signal foci just anterior and lateral to the frontal horns were found in all 56 of the selected "normal" MR scans. The foci ranged in size from punctate up to a centimeter in width (Fig. 1). They were of a uniform triangular shape, with the base resting directly on the tips of the frontal horns and with the apex pointing anteriorly into the adjacent white matter. The medial aspect of the triangle was defined by the genu of the corpus callosum, while the lateral border extended along the white matter terminating posteriorly at the head of the caudate in the most prominent cases. No size correlation with age or symptomatology was present (Fig. 2).

Histologically, the specimens exhibited three obvious findings in the region of interest: (1) decreased myelin content when compared with adjacent major white-matter tracts; (2) ependymitis granularis in the frontal horns, a condition characterized by focal breakdown of the ependymal lining and astrocytic gliosis; and (3) evidence of increased periependymal and extracellular fluid.

The region of the white matter just anterior to the frontal horns corresponding to the MR findings discussed above was unique for its relatively low myelin content. This finding was demonstrated by the decreased intensity of the blue myelin stain locally (Fig. 3). Two specific factors appeared to contribute to this finding. The first was the loose packing arrangement of the axons. In almost all white-matter tracts, the axons were ordered and tightly packed, usually in bundles (Fig. 4B). In contrast, in the area in question, the axons appeared to be "randomly" distributed (Fig. 4D). This loose distribution produced a visibly greater space between the myelinated axons.

Fig. 1.—50-year-old woman with hearing loss, referred to rule out acoustic neurinoma. TR = 2.0 sec, TE = 40 msec. Spin-echo images clearly demonstrate high-intensity foci just anterior to angle of frontal horns bilaterally.

Fig. 2.—1½-year-old female with seizures. TR = 2.0 sec, TE = 40 msec. Even at this age, high-intensity foci are clearly visible.

The second factor was the distinctly smaller size of the axons in this region. Unlike other white-matter regions, the axons in this area were more delicate and tenuous (compare Figs. 4B and 4D). A basic tenet of neurobiology states that the amount of myelin surrounding an axon is directly related to the size of the axon. Therefore, relatively little myelin surrounded the axons in the region described. In summary, both the smaller size of the myelinated axons, as well as the greater space between them, produced an obvious decrease in myelin per given volume of tissue compared with more typical regions of normal white matter.

We also noted in all the specimens a condition known as ependymitis granularis, which consists of breakdown of the ependymal lining and is distinguished from artifacts of staining or slide preparation by the underlying astrocytic gliosis [9]. The most severe involvement by ependymitis granularis in our "normal" autopsy specimens was found in the region just at the corner of the frontal horn, with observed breakdown of the ependyma extending for a short distance along the medial aspect of the frontal horn adjacent to the corpus callosum (Fig. 4A). Along the caudate, the ependymal lining was usually well preserved. This observation is supported by previous pathologic reports [10, 11].

Ependymitis granularis was found in all specimens and in all age groups. Furthermore, the degree of its severity did not correlate with age. Of note, the only specimens examined that did not demonstrate any evidence of ependymitis gran-
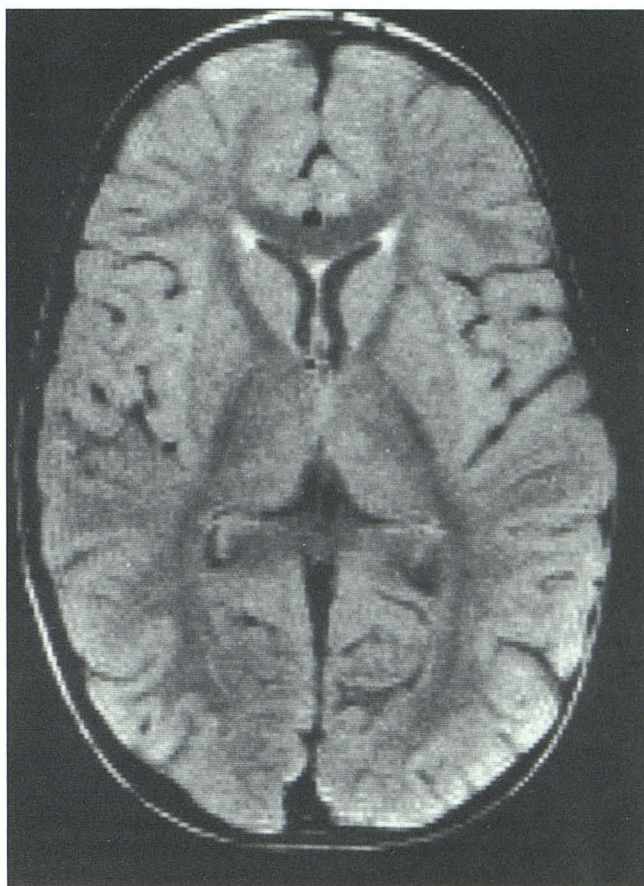
ularis were fetuses of 20 weeks gestation. The appearance of the defects in the ependymal lining correlated with the time at which the subependymal germinal matrix disappears.

Finally, increased amounts of periependymal and extracellular fluid were visualized at the dorsolateral angle of the lateral ventricles as bubblelike areas separating the axons (compare Figs. 4C and 4E). The absence of astrocytic processes indicated that these represented foci of dilated extracellular space. The greatest concentration of extracellular fluid was noted immediately adjacent to the ventricles, decreasing as one moved deeper into the brain substance. The distribution of this periventricular extracellular fluid coincided with subjacent regions of ependymal breakdown and with the increased space between the loosely arranged myelinated bundles described above. No evidence of this phenomenon was seen in a perivenular distribution, despite the fact that this region is also notable for a rich venous plexus.

Discussion

Areas of high signal intensity within normal surrounding brain tissue on T2-weighted images of spin-echo acquisitions generally indicate disease. However, in the region of the brain
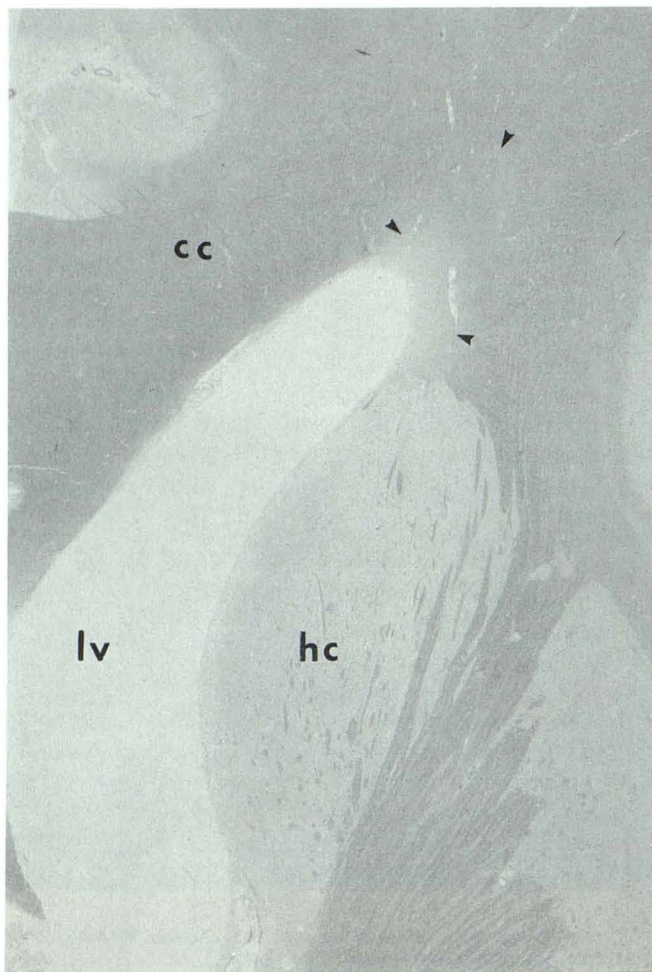
Fig. 3.—Axial brain section stained for myelin. Myelin-containing white-matter tracts are dark while gray matter is light. Note decreased myelin content (reflected by lighter shade of gray) at angle of left lateral ventricle (*arrows*). Extent of region is defined laterally and medially by white-matter tracts and posteriorly by head of caudate. These boundaries correlate well with MR appearance. (cc = corpus callosum, lv = frontal horn of lateral ventricle, hc = head of caudate) Luxol Fast Blue PAS stain, ×5.

Fig. 4.—**A**, Higher magnification of angle of frontal horn of lateral ventricle. Regions of ependymitis granularis can be identified by focal loss of ependymal lining (*arrowheads*). Note intact ependymal remnants between areas of denudation (lv = frontal horn of the lateral ventricle, cc = corpus callosum). Bielschowsky stain for axons, ×16. **B**, Axons of corpus callosum are more tightly packed and larger in this typical white-matter tract than axons in region just anterior to frontal horns. This appearance is essentially identical to that seen in other white-matter tracts e.g., the corona radiata and internal capsule, which were also examined. Bielschowsky stain for axons, ×500. **C**, Myelin stain of corpus callosum confirms increased myelin content and relative lack of extracellular space compared with region just anterior to frontal horns. Luxol Fast Blue PAS, ×500. Again, this appearance is typical of all white-matter tracts studied. **D**, Axonal stain from region anterior to frontal horns reveals axons that are both tenuous and loosely packed. Bielschowsky stain for axons, ×500. **E**, Myelin stain of same region as D confirms increased extracellular space, seen as unstained regions separating darkly staining myelin strands. Luxol Fast Blue PAS, ×500.

discussed here, histologic evidence that explains the increased intensity has been found. An elevated water content can be demonstrated and most likely explains the finding on MRI. Multiple factors combine to raise the hydration in this area of the white matter. Myelin is hydrophobic and is composed of only 40% water, with the remaining fraction taken up by lipid (45%) and protein (15%). This fact accounts for the relatively smaller water concentration in white matter (70%–75%) as compared with gray matter (83%) [12]. The presence of relatively small axonal bundles with greater space between them endows the locus of white matter just anterior to the frontal horns with a relatively lower content of the hydrophobic myelin and allows more hydration.

Another cause of increased extracellular fluid in this region, especially in the periependymal area, may well be ependymitis gran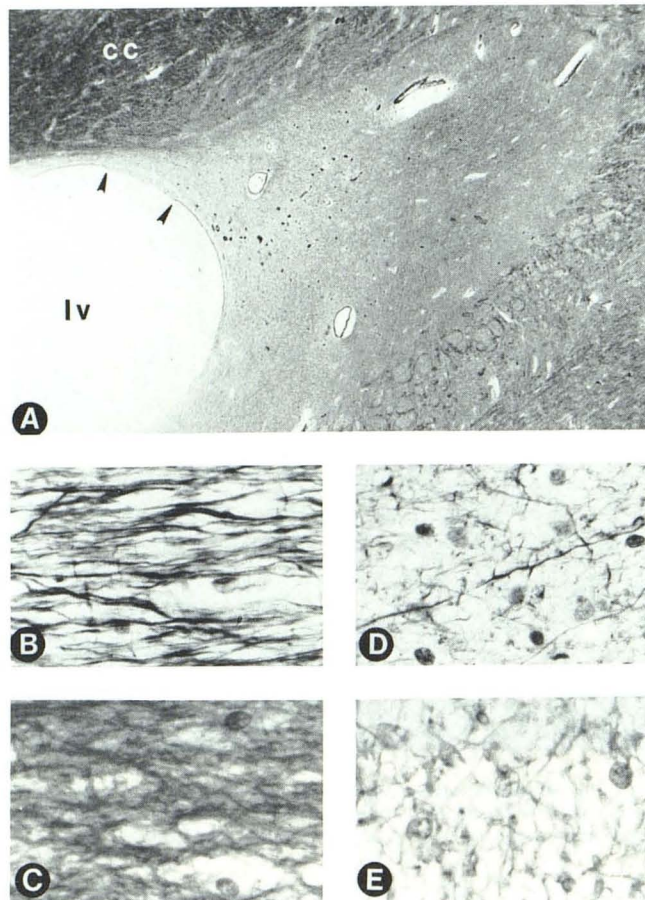ularis. Observations of certain pathologic states provide insight into the mechanism of this MR finding. In hydrocephalus, as the ventricular surface expands, the ependymal cells become flattened and stretched, followed by frank denudation [9, 11]. This process facilitates entry of cerebrospinal fluid into the tissue, since the ependymal cells are no longer present to regulate fluid exchange between the ventricles and the brain substance [13, 14, 15]. Although this breakdown of the ependymal lining in hydrocephalus or inflammation also leads to ependymitis granularis, it differs from the disruption that was seen in the normal specimens described here both in its much greater extent and in its obvious pathologic origin. Previous pathology literature has also described localized

ependymitis granularis in normal autopsy specimens [10, 16, 17]. One can speculate that such ependymal breakdown at the tips of the frontal horns may augment the accumulation of extracellular fluid in this specific region, just as it does on a global basis in hydrocephalus. Some pathologists have observed that localized breakdown of the ependyma is almost universal, even by late fetal life. Dooling et al. [10] demonstrated focal ependymal loss in the same region of the frontal horns in 85% of fetuses more than 35 weeks old. They also mentioned similar findings near the occipital horn angle. High-intensity foci on MR images are occasionally seen in the occipital horn, even in young patients, although accurate assessment of this area is slightly more difficult owing to the high intensity of the adjacent choroid plexus and the variable size and posterior extension of the occipital horn. Disruption of the ependyma has not been described in normal specimens in the third or fourth ventricles [17].

The etiology of localized ependymitis granularis is unclear. This phenomenon, repeatedly noted and consistent in both location and extent, may result from the normal process of development and may be secondary to the molding necessitated by the increasing size and complexity of the growing brain. In addition, pulsatile hydrostatic forces of the cerebrospinal fluid may also play a role [10]. Interestingly, the localized ependymitis granularis occurs in the cerebral regions that contain the last vestiges of the subependymal germinal matrix. In our specimens, the time of appearance of the breakdown of the ependyma coincided with the disappearance of these primitive neuroepithelial cells. The significance of this temporal relationship is unknown.

Finally, previously reported studies of cerebrospinal fluid dynamics and formation provide another explanation for the increased local collections of periependymal fluid that we visualized. Investigations of fluid pathways indicate that interstitial fluid in the brain substance follows preferential drainage routes to the subependymal region, especially to the dorsolateral angle of the lateral ventricle [18, 19]. Cserr et al. found that labeled anionic horseradish peroxidase injected into the caudate nucleus of rats had a propensity to flow to the region of the brain just anterior to the frontal horns. Thus it appears that this region serves as a natural funnel for extracellular fluid produced in the brain interstitium, an organ devoid of deep hemispheric lymphatics. The extent and significance of these fluid pathways is considerable, because interstitial flow of fluid from the brain into the ventricles is thought to be a primary source of extrachoroidal cerebrospinal fluid formation, which has been estimated to constitute from 30% to 70% of total cerebrospinal fluid production [20, 21].

In addition, data exist that the ependymal lining functions not only as a barrier to the entry of cerebrospinal fluid into the brain substance but may also actively transport interstitial fluid out of the brain and into the ventricles [21]. When disruption of the ependyma occurs, one may speculate that the natural fluid drainage to the angle of the frontal horn may no longer be taken up and elaborated into cerebrospinal fluid and thus accumulates in these regions.

In summary, the combination of the decreased myelin content, the localized ependymitis granularis, and the natural fluid drainage pathways of the brain increases the water content focally in the region of the brain just anterior to the frontal horns. The increased water content, in turn, leads to lengthening of T1 and T2 and produces the appearance of foci of high intensity on T2-weighted spin-echo images [22].

Radiologically, the foci of high signal intensity described here are significant in that they can be confused with several pathologic processes, especially multiple sclerosis or other demyelinating disorders, subcortical arteriosclerotic encephalopathy, hydrocephalus, and changes of radiation therapy.

Multiple sclerosis (MS) is the most important pathologic entity to consider in the differential diagnosis because of its predilection for the lateral-ventricular angles. Subependymal periventricular demyelination is classic in MS, especially contiguous to the frontal and occipital horns, and is seen in approximately 90% of cases [23]. Because MS plaques are invariably perivenular, the richness of the venous plexus in the location we studied may help explain why MS so often affects this same region. Another hallmark of MS is the relative symmetry of bilateral distribution.

For the above reasons, early differentiation of MS from the normal finding described here may be difficult, especially since initial plaques are often microscopic in size. However, certain differences will appear, especially as the disease progresses. Even if the plaques are confined to the periventricular region near the frontal horn, they do not respect the boundaries of the high-intensity foci described earlier (Fig. 5A). As the plaques coalesce, extension into surrounding structures—for example, the corpus callosum or other adjacent white-matter tracts—is the rule rather than the exception [24]. Furthermore, distinct lesions may often extend along the entire lateral aspects of the lateral ventricles in a classic "lumpy-bumpy" pattern [2].

Pathologically, MS differs strikingly from the normal histologic appearances anterior to the frontal horn, despite possible similarities of MR appearance. In MS, one sees a remarkable punched-out, ragged appearance of demyelination, in contrast to the normal findings of decreased myelin content that we described (Fig. 5C). Furthermore, in MS the spaces between demyelinated axons become entirely filled with densely packed astrocytic processes.

Subcortical arteriosclerotic encephalopathy is another important entity to differentiate from the normal foci of high intensity. As in multiple sclerosis, subcortical arteriosclerotic encephalopathy is characterized by multiple patchy periventricular lesions [4, 25–27] (Fig. 6). Although these lesions are periventricular, many are often not immediately adjacent to the ependymal surface. In contrast, the high-intensity foci that we have described are triangular-shaped structures that rest directly on the tips of the frontal horns, both radiographically and pathologically. Furthermore, changes of subcortical arteriosclerotic encephalopathy are often associated with cortical atrophy, ventricular dilatation, and lacunar infarcts in the basal ganglia [26, 28]. Finally, these lesions may vary markedly in size and distribution.

Pathologically, subcortical arteriosclerotic encephalopathy differs from our findings in normal autopsy specimens. Elderly patients with periventricular white-matter disease noted on
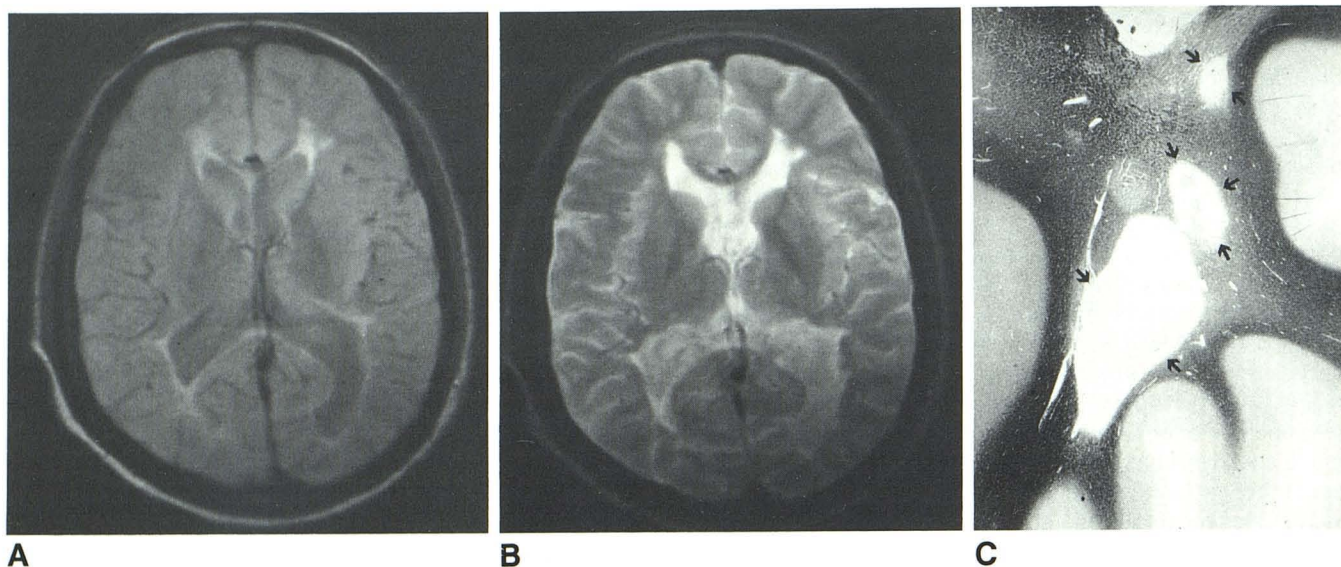
A

B

C

Fig. 5.—**A** and **B**, 43-year-old woman with a 21-year history of classic multiple sclerosis. TR = 2.0 sec, TE = 40, 80 msec. Typical extension of high-intensity lesions into adjacent white matter beyond the confines of high-intensity foci of normal scans. **C**, Myelin stain of multiple sclerosis plaques, delineated by *arrows*. Increased water content of multiple sclerosis plaque is caused in part by striking, well-defined total demyelination, as seen in this typical plaque. In contrast, axons beyond frontal horn tip are not demyelinated (see 4E).
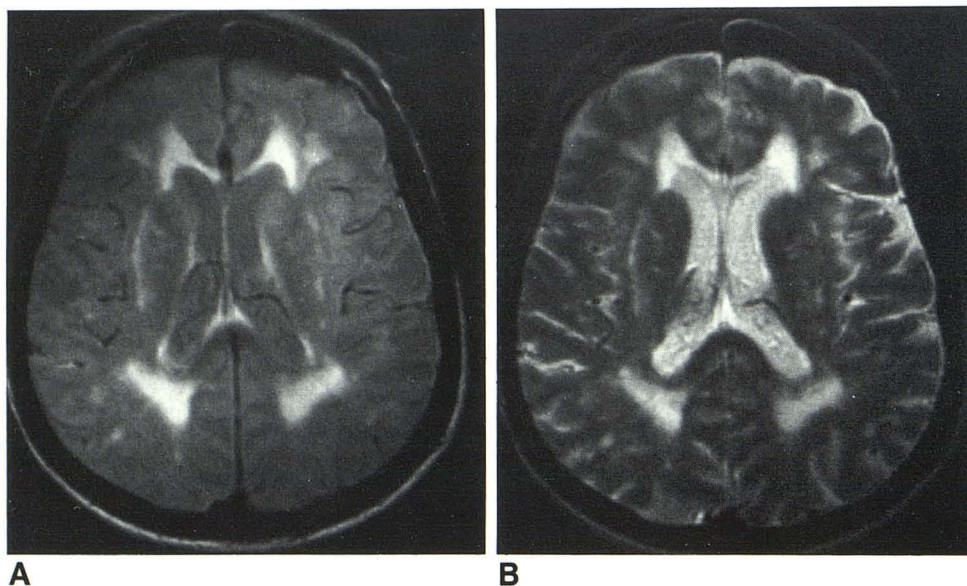
Fig. 6.—**A** and **B**, 76-year-old woman with memory loss and confusion. TR = 2.0 sec, TE = 40, 80 msec. MR scan is consistent with subcortical arteriosclerotic encephalopathy. Again, extension of high-intensity foci beyond normal boundaries is visualized, as well as multiple other foci near occipital horns and in deep white matter.

A

B

CT scans have been found to have severe arteriosclerotic changes in the deep perforating arteries to the white matter, which forms a watershed zone between the deep medullary and superficial cortical circulations [5, 29]. Thus these patients are prone to repeated small infarcts, and it is likely that this is the pathologic basis for the regions of high signal intensity seen on MR scans in these patients, although direct pathologic confirmation is still lacking.

In conclusion, foci of high signal intensity at the frontal horns are normal findings in all T2-weighted spin-echo magnetic resonance scans, and a histologic basis for them can be demonstrated. These foci do not constitute pathology in and of themselves, even though superficially they may resemble common pathologic states, such as multiple sclerosis, subcortical arteriosclerotic encephalopathy, hydrocephalus, and changes of radiation therapy.

REFERENCES

1. Brant-Zawadzki M, Norman D, Newton TH, et al. Magnetic resonance of the brain: the optimal screening technique. *Radiology* **1984**;152:71–77

2. Runge VA, Price AC, Kirshner HS, Allen JH, Partain CL, James AE Jr. Magnetic resonance imaging of multiple sclerosis: a study of pulse-technique efficacy. *AJNR* **1984**;5:691–702, *AJR* **1984**;143:1015–1026

3. Vermess M, Bernstein RM, Bydder GM, Steiner RE, Young IR, Hughes GRV. Nuclear magnetic resonance imaging of the brain in systemic lupus erythematosus. *J Comput Assist Tomog* **1983**;7(3):461–467

4. Erkinjuntti T, Sipponen JT, Iivanainen M, Ketonen L, Sulkava R, Sepponen RE. Cerebral nuclear magnetic resonance and computed tomography imaging in dementia. *J Comput Assist Tomog* **1984**;8(4):614–618

5. Zeumer H, Schonsky B, Sturm KW. Predominant white matter involvement in subcortical arteriosclerotic encephalopathy (Binswanger disease). *J Comput Assist Tomog* **1980**;4(1):14–19

6. Brant-Zawadzki M, Davis PL, Crooks LE, et al. Nuclear magnetic resonance demonstration of cerebral abnormalities: comparison with computed tomography. *AJNR* **1983**;4:117–124, *AJR* **1983**;140:847–854

7. Crooks L, Arakawa M, Hoenninger J, et al. Nuclear magnetic resonance whole-body imager operating at 3.5 Kilogauss. *Radiology* **1982**;143:169–174

8. Crooks LE, Mills CM, Davis PL, et al. Visualization of cerebral and vascular abnormalities by nuclear magnetic resonance imaging: the effects of imaging parameters on contrast. *Radiology* **1982**;144:843–852

9. Russell DS. Observations on the pathology of hydrocephalus. In: *Special report series*, No. 265. London: Med Res Council, **1949**

10. Dooling EC, Chi JG, Gilles FH. Developmental changes in ventricular epithelia. In: Gilles FH, Leviton A, Dooling EC, *The developing human brain: growth and epidemiologic neuropathology*. Boston, Bristol, London: John Wright, **1983**:113–116

11. Page RB, Rosenstein JM, Dovey BJ, Leure-DuPree AE. Ependymal changes in experimental hydrocephalus. *Anat Rec* **1979**;194:83–103

12. Brooks RA, DiChiro G, Keller MR. Explanation of cerebral white-gray contrast in computed tomography. *J Comput Assist Tomog* **1980**;4:489–491

13. Brightman MW, Reese TS. Junctions between intimately opposed cell membranes in the vertebrate brain. *J Cell Biol* **1969**;40:648–677

14. Hochwald GM, Lux WE Jr, Sahar A, Ransohoff J. Experimental hydrocephalus: changes in cerebrospinal fluid dynamics as a function of time. *Arch Neurol* **1972**;26:120–129

15. Milhorat TH, Clark RG, Hammock MK, McGrath PP. Structural, ultrastructural, and permeability changes in the ependyma and surrounding brain favoring equilibration in progressive hydrocephalus. *Arch Neurol* **1970**;22:397–407

16. Banker BQ, Larroche J-C. Periventricular leukomalacia of infancy. *Arch Neurol* **1962**;7:386–410

17. Friede RL. *Developmental neuropathology*. New York, Vienna: Springer-Verlag, **1975**:11–13

18. Bertrand C. Diffusion and absorption in the brain. *Exp Neurol* **1952**;11:53–61

19. Cserr HF, Cooper DN, Milhorat TH. Flow of cerebral interstitial fluid as indicated by the removal of extracellular markers from rat caudate nucleus. *Exp Eye Res* [Suppl to Vol. 25, Fogarty International Center Symposium] **1977**:461–473

20. Hochwald GM, Wald A, Malhan C. The sink action of cerebrospinal volume flow. *Arch Neurol* **1976**;33:339–344

21. Pollay M, Curl F. Secretion of cerebrospinal fluid by ventricular ependyma of the rabbit. *Am J Physiol* **1967**;213:1031–1038

22. Brant-Zawadzki M, Bartkowski HM, Pitts LH, et al. Nuclear magnetic resonance imaging of experimental and clinical cerebral edema. *Noninvasive Med Imaging* **1984**;1:43–47

23. Lumsden CE. The neuropathology of multiple sclerosis. In: Vinken PJ, Bruyn GW, eds., *Handbook of clinical neurology. MS and other demyelinating diseases*, Vol. 9. Amsterdam, New York: American Elsevier, **1970**:217–309

24. Johnson MA, Li DKB, Bryant DJ, Payne JA. Magnetic resonance imaging: serial observations in multiple sclerosis. *AJNR* **1984**;5:495–499

25. Bradley WG, Waluch V, Brant-Zawadzki M, Yadley RA, Wycoff RR. Patchy peri-ventricular white matter lesions in the elderly: a common observation during NMR imaging. *Noninvasive Med Imaging.* **1984**;1:35–41

26. Kinkel WR, Jacobs L, Polchini I, Bates V. Late onset sub-cortical encephalopathy: computed tomography, nuclear magnetic resonance, and clinical correlations. American Neurological Association Meeting, New Orleans, October **1984**

27. Young IR, Randell CP, Kaplan PW, James A, Bydder GM, Steiner RE. Nuclear magnetic resonance imaging in white matter disease of the brain using spin-echo sequences. *J Comput Assist Tomog* **1983**;7(2):290–294

28. Le May M. Radiologic changes of the aging brain and skull. *AJNR* **1984**;5:269–275, *AJR* **1984**;143:383–389

29. Goto K, Ishii N, Fukasawa H. Diffuse white matter disease in the geriatric population. *Radiology* **1981**;141:687–695